



Terrestrial Signature of a Recently-Tidewater Glacier and Adjacent Periglaciation, Windy Glacier (South Shetland Islands, Antarctic)

Kacper Kreczmer¹, Maciej Dałbski^{2*} and Anna Zmarz³

¹ College of Inter-faculty Individual Studies in Mathematics and Natural Sciences, University of Warsaw, Warsaw, Poland,

² Faculty of Geography and Regional Studies, Department of Geomorphology, University of Warsaw, Warsaw, Poland,

³ Faculty of Geography and Regional Studies, Department of Geoinformatics, Cartography and Remote Sensing, University of Warsaw, Warsaw, Poland

OPEN ACCESS

Edited by:

Jesús Rodrigo-Comino,
Universität Trier, Germany

Reviewed by:

Enrique Serrano,
University of Valladolid, Spain
Kátia Kellem Rosa,
Federal University of Rio Grande do
Sul, Brazil

*Correspondence:

Maciej Dałbski
mfdabski@uw.edu.pl

Specialty section:

This article was submitted to
Environmental Informatics
and Remote Sensing,
a section of the journal
Frontiers in Earth Science

Received: 24 February 2021

Accepted: 07 April 2021

Published: 29 April 2021

Citation:

Kreczmer K, Dałbski M and
Zmarz A (2021) Terrestrial Signature
of a Recently-Tidewater Glacier
and Adjacent Periglaciation, Windy
Glacier (South Shetland Islands,
Antarctic). *Front. Earth Sci.* 9:671985.
doi: 10.3389/feart.2021.671985

Contemporary retreat of glaciers is well visible in the West Antarctic region. The aim of this study is to identify, map and quantify terrestrial glacial and periglacial landforms developed in front of Windy Glacier (Warszawa Icefield, King George Island, South Shetlands), which recently turned from being tidewater to land-terminating, and on nearby Red Hill. The study is based on an orthophoto map and a DEM elaborated with a use of images obtained during a UAV BVLOS photogrammetric survey in 2016, Google Earth Pro images from 2006 and an orthophoto map from 1978/1979. The geomorphological map obtained includes 31 types of landforms and water bodies, grouped into: (1) glacial depositional landforms, (2) fluvial and fluvio-glacial landforms, (3) littoral and lacustrine landforms, (4) solifluction landforms, (5) other mass movement landforms, (6) patterned ground, (7) debris flows, landslides and mudflows, (8) water bodies, (9) other (bedrock, boulders, glacial ice, snow patches, and not recognized surface). Most area is occupied by glacial lagoon, fluvial and fluvio-glacial landforms, not recognized surfaces and littoral landforms. Between 2006 and 2016 the glacier deposited a well-developed patch of fluted moraine with small drumlins. We recognize the glacial-periglacial transition zone between 41 and 47 m GPS height above which solifluction landforms and sorted patterned ground dominate. Advantages of UAV and BVLOS missions are highlighted and problems with vectorization of landforms are discussed. Distinction between flutes and small drumlins is shown on length-to-elongation and length-to-width diagrams and critical reference to previous geomorphological mappings on King George Island is presented.

Keywords: glacial landforms, periglacial landforms, King George Island, Antarctic, unmanned aerial vehicles, glacial recession, photointerpretation

INTRODUCTION

Contemporary retreat of glaciers (World Glacier Monitoring Service [WGMS], 2020), well visible in alpine environments and in the Arctic is also significant in the West Antarctic region, including Antarctic Peninsula and South Shetland Islands (Cook et al., 2005; Meredith and King, 2005; Turner et al., 2014). Antarctic ecosystems, frequently protected as the

Antarctic Specially Protected Areas (ASPAs) are now subject to rapid transformation which influences wildlife and the source-to-sink sediment budgets (Zwoliński et al., 2016; Lee et al., 2017; Znój et al., 2017). New ice-free oases are developed due to recent on-shore termination of formerly tidewater glaciers. The southern and eastern margins of the Warszawa Icefield (Figure 1) on King George Island (KGI), South Shetland Islands, are also subjected to retreat which transformed tidewater glacial fronts to land-terminating ones and liberated from glacial ice over 6 km² since the first general survey in 1979 (Pudelko, 2003; Pętllicki et al., 2017; Pudelko et al., 2018; Da Rosa et al., 2020).

The development of the terrestrial glacial landforms in front of the retreating glacier and periglacial phenomena in this area received considerable attention since the end of the 20th century due to the nearby location of the Henryk Arctowski Polish Antarctic Station (Arctowski) (Birkenmajer, 1980; Dutkiewicz, 1982; Kostrzewski et al., 1998, 2002; Rachlewicz, 1999). Satellite and conventional aerial imagery recently allowed for deepening our understanding of glacial dynamics and gave some information on the rate of development of glacial landforms (Pętllicki et al., 2017; Pudelko et al., 2018; Sziło and Bialik, 2018; Da Rosa et al., 2020), however, they sometimes lead to improper interpretations.

In years 2014–2016 the MONICA project (A novel approach to monitoring the impact of climate change on Antarctic ecosystems) was realized in the area of Arctowski, which utilized unmanned aerial vehicle (UAV) platforms and Beyond Visual Line of Sight (BVLOS) operations. The project resulted in three geomorphological studies so far, including: periglaciation of Demay Point (Dąbski et al., 2017), general morphology of

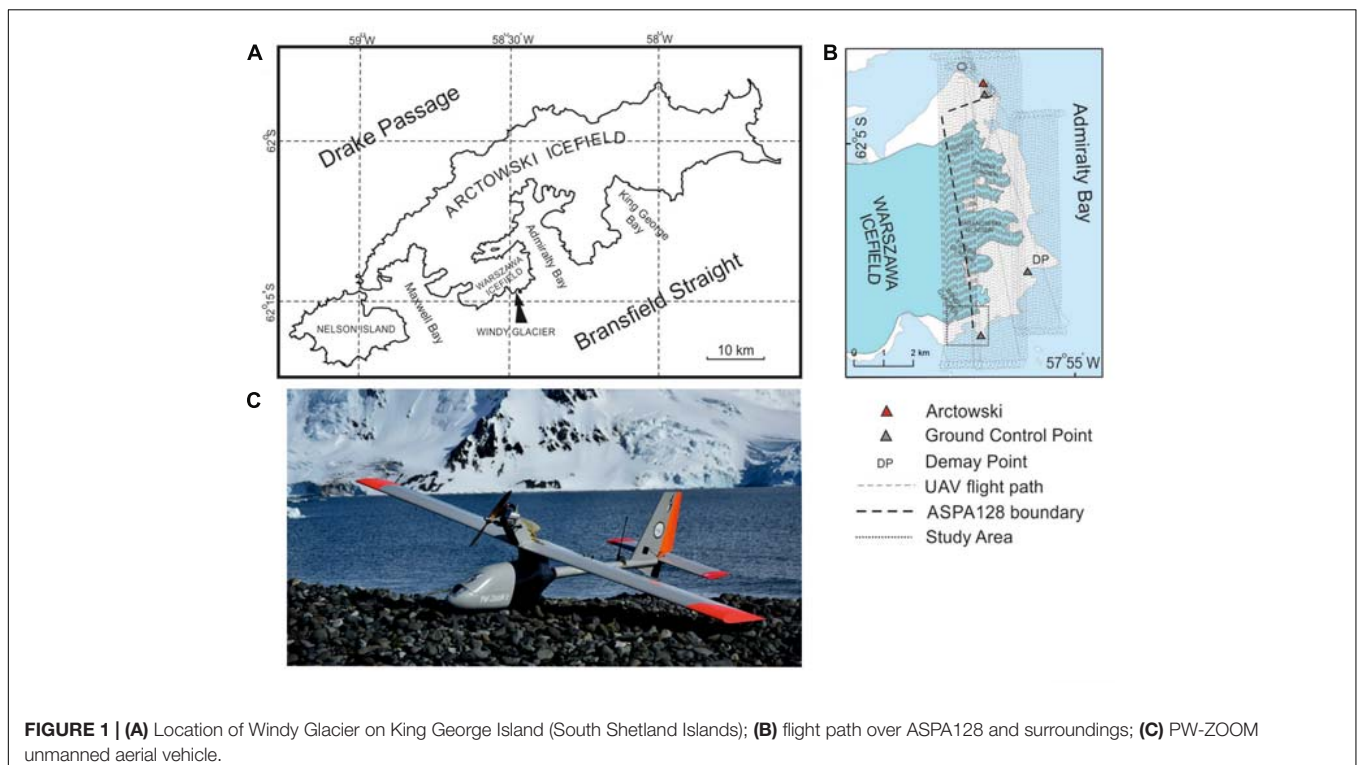
Penguin Island (Zmarz et al., 2018) and development of forelands of Ecology, Sphinx and Baranowski glaciers (Dąbski et al., 2020). However, the foreland of near-by Windy Glacier (Figure 1) was omitted, due to its marginal location and relatively small size of the foreland.

The aim of this study is to fill this gap by identification, mapping and quantification of terrestrial glacial and periglacial landforms developed in front of Windy Glacier, which recently turned from being tidewater to land-terminating. The analysis of the landform assemblages allowed to infer about the glacial dynamics and the significance of contemporary periglacial processes developed in the adjacent area. Moreover, we critically address the previous geomorphological mapping of the area under study based on satellite images (Da Rosa et al., 2020).

The research was based on a high-resolution orthophoto map and a digital elevation model (DEM) created by A. Zmarz on the basis of images obtained during a photogrammetric survey performed over the west coast of Admiralty Bay in 2016. The mapping was not confirmed in the field by checking the internal structure of landforms, however, identified landforms were sufficiently visible of the aerial images to allowed for relatively detailed geomorphological interpretation.

Location, Climatic and Geological Setting of the Windy Glacier Foreland

Windy Glacier is located at the southern boundary of the Antarctic Specially Protected Area No. 128 (ASPAs 128) which covers the west coast of Admiralty Bay in the vicinity of Arctowski (Figures 1A,B). Glacial recession in ASPA 128 since 1979 was documented by Pudelko et al. (2018), and the general



geomorphological mapping the forelands of Ecology Glacier, Sphinx Glacier and Baranowski Glacier (main glaciers of ASPA 128) was recently performed by Dąbski et al. (2020).

Bedrock of the area includes basaltic (tholeiites) and andesitic lavas interbedded with Eocene–Oligocene sediments and volcanic plugs and dikes of Pleistocene age (Birkenmajer, 1980). Quaternary sediments are represented by glacial and fluvio-glacial sediments, periglacial, weathering and mass-movement sediments as well as marine sands and gravels (Birkenmajer, 1981; Rachlewicz, 1999; Kostrzewski et al., 2002).

Mean annual air temperature (MAAT) in the study area is -1.5°C , rainfall or snowfall occur throughout most of the year, and snow cover is highly variable, redistributed by strong winds (Dutkiewicz, 1982; Gonera and Rachlewicz, 1997; Robakiewicz and Rakusa-Suszczewski, 1999; Marsz and Styszyńska, 2000; Wierzbicki, 2009; López-Martínez et al., 2012; Kejna et al., 2013; Zwoliński et al., 2016). Polar maritime climate of the area is responsible for highly dynamic weather conditions which are demanding for any UAV operations and for photointerpretation of medium- to small-scale landforms or margins of glaciers which can be covered by snow drift. Climatic changes observed since the onset of instrumentalization in this area (MAAT in years 1948–2011 increased by 1.2°C), results in glacial recession, disappearance of permafrost from coastal areas and inactivation of certain large-scale periglacial landforms (Dąbski et al., 2017, 2020; Pudełko et al., 2018). However, since the beginning of the 21st c. regional cooling is observed (Oliva et al., 2016) which is responsible for slowing deglaciation rates or glacial still-stands.

Windy Glacier flows SE of the Warszawa Icefield (max elevation 450 m a.s.l.) and its equilibrium line altitude varied between 140 m a.s.l. and 290 m a.s.l. in years 1979–2018 (Pudełko et al., 2018). Ice thickness in the frontal part of the glacier does not exceed 100 m, and ice flow velocity is below 100 m year^{-1} (Osmanoğlu et al., 2013). Dąbski et al. (2020) concluded that the neighboring glaciers in ASPA 128 probably experienced discontinuous fast ice flow typical of tidewater glaciers. Recent contact of the Windy Glacier with the lagoon, allowed for more dynamic behavior of the glacier by allowing for calving. Thermal state of the glacier is unknown, and both polythermal and temperate glaciers are present on KGI (Benjumea et al., 2003; Young Kim et al., 2010). According to Da Rosa et al. (2020) during 1979–2018 Windy Glacier area loss amounted to 1.10 km^2 (31% of 3.51 km^2 in 1979). The rate of deglaciation decreased in years during the 2000–2018 due to climatic cooling and the transition of glacier margin from tidewater to land-terminating.

Tidal range of about 1.5 m (Robakiewicz and Rakusa-Suszczewski, 1999) results in a well-developed beach, coastal cliffs and a glacier lagoon in the Windy Glacier foreland. The lagoon played a significant role in shaping the glacier's dynamics before 2006, but afterward the glacier underwent a transformation from tidewater to land-terminating.

The western and southern margins of the Warszawa Icefield, including the Windy Glacier foreland, constitute a lowland ice-free area (about 16.8 km^2), covered by diverse tundra communities (Chwedorzewska and Bednarek, 2011) suitable for huge breeding colonies of marine birds and pinnipeds

(Sierakowski et al., 2017), e.g., on Patelnia Point (**Figure 2**) near the Windy Glacier margin (Fudala and Bialik, 2020).

METHODS

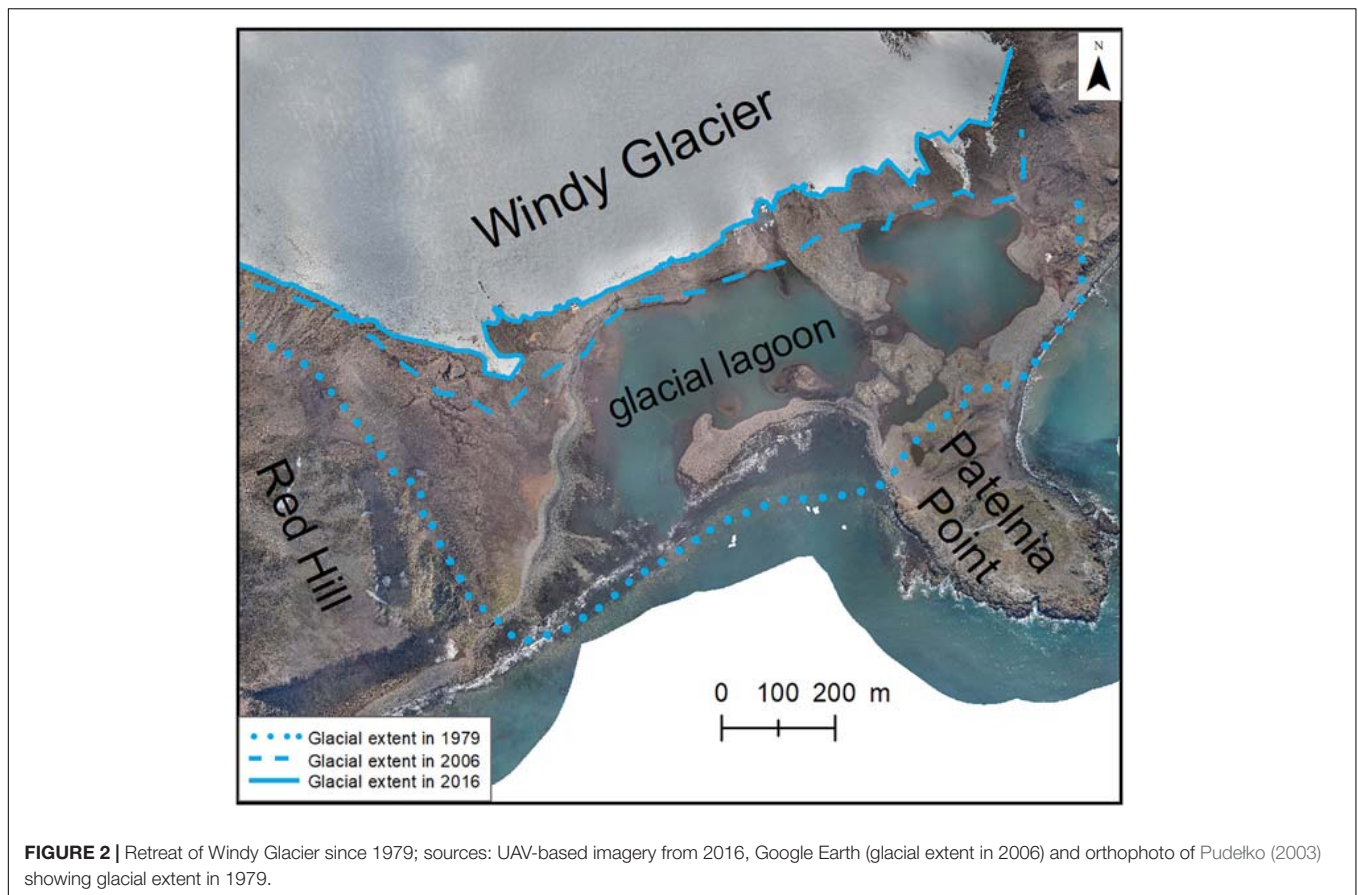
Data Acquisition

During realization of the MONICA project a photogrammetric survey was performed over ASPA 128 on 15–17 November 2016 with a use of a PW-ZOOM fixed-wing UAV and a BVLOS operation (**Figures 1B,C**). The UAV was designed especially for polar conditions and manufactured in the Warsaw University of Technology (Goetzendorf-Grabowski and Rodzewicz, 2017; Rodzewicz et al., 2017). The starting and landing points of the PW-ZOOM were located near Arctowski. An automatic control system linked with a telemetry module in the Ground Control Station (GSC), connected to a computer running HORIZONmp software allowed for a fully autonomous flight. The flight path lines were spaced circa 70 m apart, which provided 70% forward and side overlap and flight altitude was 500 m a.s.l. The images were gathered in three flights 7 h in total, covering a distance of 720 km. All images obtained had georeferences (X, Y, Z) registered by the autopilot logger mounted on the UAV. The GPS Receiver GP-E2 was used for geolocation of the images allowing for horizontal accuracy of measurement $<5\text{ m}$. GPS measurements of three ground control points (GCP), marked in **Figure 1B**, were used to determine the vertical accuracy (accuracy of measurement was $<2\text{ m}$).

Other sources of aerial imagery used in this study included Google Earth Pro (GE) images from 2006 and an orthophoto map based on aerial photography from 1978/1979 (Pudełko, 2003). The GE images obtained were of relatively low resolution (1.7 m), but they allowed to get valid data on the glacier margin position in 2006, because the glacier margin was clearly visible against characteristic foreland features (**Figure 2**).

Data Processing

Images obtained with the use of the UAV platform were processed into an orthophoto with a resolution of 0.06 m (**Figure 2**) and a DEM of 0.25 m resolution in the WGS84 coordinate system (**Supplementary Figure 1**) showing elevation in meters GPS height (m GPS h.). The orthophoto map and DEM were created with use of the Agisoft Metashape Professional software (Version 1.3.2) and the Structure from Motion (SfM) algorithm. The orthophoto was converted to UTM system in ESRI ArcGIS 10.3 software. Google Earth satellite images (from 2006) were georeferenced in ESRI ArcGIS to the WGS84 coordinate system, the same as one used in the orthophoto map (**Figure 2**). The root mean square error (RMSE) was 1.46 m. The orthophoto and DEM (**Supplementary Figure 1**) allowed to manually determine boundaries of landforms or patches of land surface exhibiting uniform morphological characteristics (e.g., sorted circles) by vectorization in ESRI ArcGIS 10.3 software at scales between 1:500 and 1:2000 (**Figure 3** and **Supplementary Figures 2, 3**). The length-to-elongation ratio diagram allowed for distinction between flutes and drumlins (**Figure 4**).



RESULTS

Windy Glacier is a thin and short glacier lobe filling a shallow glacier trough which delivered the ice to the open sea until 1979 (Figure 2). There are no terrestrial Little Ice Age (LIA) terminal moraine ridges, because the glacier terminated in the sea in the LIA maximum. The oldest end moraine complex (recessional moraine ridges) is deposited on the Patelnia Point (Figures 2, 3) and should be associated with the 20th century still-stands or short advances (see Discussion). Well-developed beaches and storm ridges can be found along the coastline and a strip of a shallow coastal cliff cut in bedrock is visible along the shore of Patelnia Point.

The following glacial retreat resulted in a creation of the glacial lagoon which now is composed of two main water bodies and constitutes most of the glacial foreland – almost 23% of study area (Figures 2, 3). Apart from the lagoon, the area liberated from glacier ice between 1979 and 2006 is characterized by a well-developed alluvial fan (sandur) west of the lagoon and a large relatively flat “not recognized surface” (Figure 3).

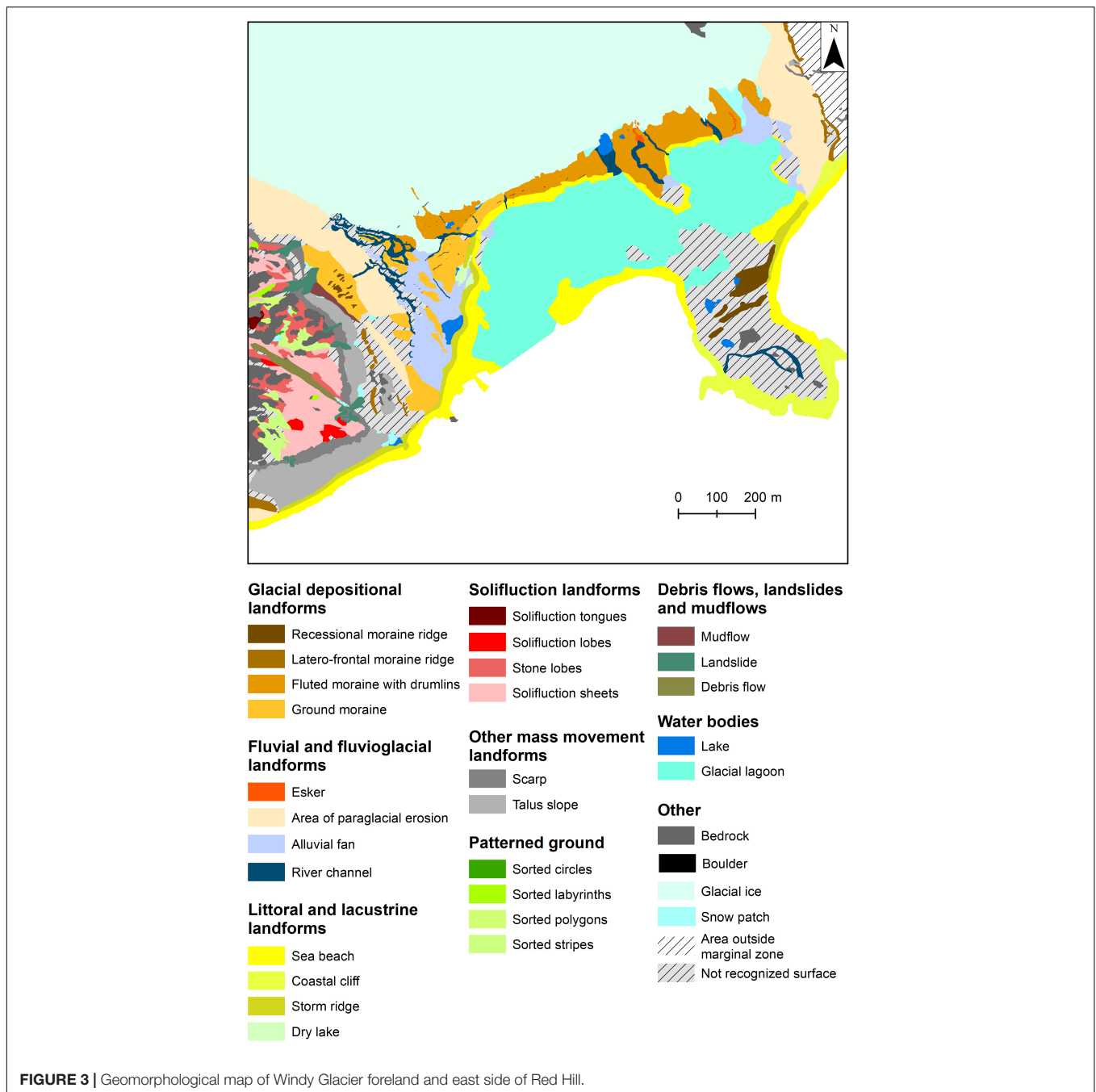
The interior part of the glacier foreland, deglaciated after 2006 (Figure 2), is dominated by the ground moraine with small recessional moraine ridges, especially in its western part (close to Red Hill foothills), as well as small drumlins and flutes – fluted moraine with a direct contact with the glacier (Figures 3, 4 and Supplementary Figure 3). The area is dotted with erratic

boulders, some exceeding 1 m in diameter, and dissected by river channels up to 15 m wide and 6 m deep. Most of them were dry during the photogrammetric flight.

Among mapped fluvial and fluvio-glacial landforms, we distinguished a large area of paraglacial erosion which is a surface built with glacial sediments (*sensu largo*) and heavily dissected by small gullies and rills (Figure 3). The area of paraglacial erosion is best developed on foothills of the glacial trough, most probably covered by glacial drift. Two narrow latero-frontal moraine ridges are developed, one along the eastern upper edge of the glacial trough (directly above the area of paraglacial erosion), and another one at foothills of taluses deposited on the eastern slopes of Red Hill. There is also a significant area (16% of the study area) of “not recognized surface” in terms of morphogenesis due to the lack of characteristic indicative morphological features (Figure 3).

There is no clear-cut periglacial trimline, because we do not observe the abrupt boundary between the ground shaped predominantly by freeze-thaw processes and the erosional or depositional glacial landforms. However, we can determine a glacial-periglacial transition zone between the lowest limit of periglacial landforms (the lowest reach of solifluction landforms – 47 m GPS h.) and the upper limit of glacial landforms (the uppermost reach of the lateral moraine ridge – 41 m GPS h.).

Periglacial phenomena are restricted to upper part of Red Hill (Figures 2, 3), above the upper edge of the scarp located



at 70–90 m GPS h. (**Supplementary Figure 1**). Most of this area is covered by solifluction landforms, especially solifluction sheets (3.95 ha). Among patterned ground, sorted stripes prevail (1.05 ha) and sorted circles occupy the smallest area (0.02 ha).

DISCUSSION

Methodological Considerations

Results of our large-scale geomorphological mapping of Windy Glacier foreland disagrees with the small-scale mapping of the

same area performed by Da Rosa et al. (2020) based solely on satellite images. For example, stretches of beach are interpreted in the mentioned study as recessional moraine ridges, and a very well visible recessional moraine complex on Patelnia Point (**Supplementary Figure 1** and **Figure 3**) is not mapped by Da Rosa et al. (2020). Furthermore, the referenced study depicts three zones in terms of proglacial geomorphic activity: (i) zone of high activity (deglaciated in years 2000 – 2018, characterized by intensive paraglacial susceptibility), (ii) zone of moderate activity, deglaciated in years 1970s – 2000, and (iii) zone of low activity, deglaciated before 1970. We question the validity

of the zonation in terms of dating and paraglacial activity. This is because contemporary intensive rilling and gulying can be seen on a slope in the western part of the foreland, immediately below the latero-frontal moraine ridge, deglaciated since 1979 (Figures 2, 3). However, this area was labeled by Da Rosa et al. (2020) as the low activity zone, deglaciated before 1970s.

Similar, the periglacial investigation of López-Martínez et al. (2012) for South Shetland Islands based on relatively small-scale aerial photographs and satellite imagery did not take into account small ice-free areas on KGI such as Demay Point (Figure 1B) or Red Hill. This shows that the high-resolution images, e.g., obtained with the use of a UAV platform, is much more suited for detailed geomorphological studies. In many cases, the UAV BVLOS operations constitute a very good solution to reach remote locations and to provide security for the researchers.

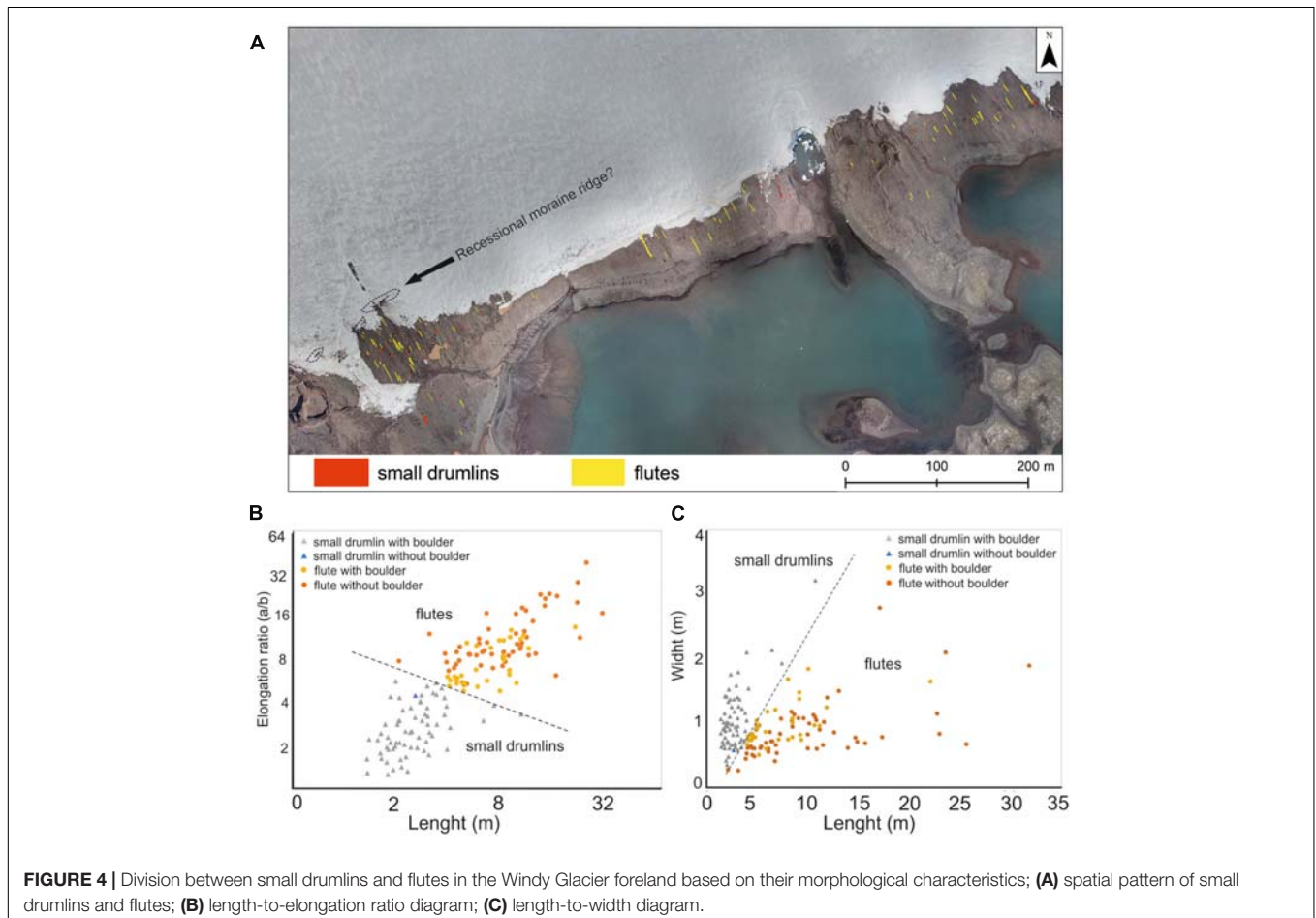
Vectorization in GIS software can be easily performed on high-resolution orthophoto showing landforms which have easily distinguishable boundaries (e.g., sorted stripes, fluted moraine, and recessional moraine ridges), but it can be problematic when sorted polygons or solifluction sheets are delimited due to the lack of clear-cut morphological boundaries (Supplementary Figure 2). This is a source of a potential error in our mapping, however, this problem occurs also when field-based methods of mapping are used. Probably it neither would be overcome

by machine learning, because at the end, manual identification would be necessary to validate the automatic mapping.

Certain small landforms can be relatively well visible but difficult to interpret based solely on the orthophoto map, because of snow or ice cover masking the full picture. In the western part of the Windy Glacier, inside the white surface (interpreted as glacier ice) we noticed a small and fragmented ridge running perpendicular to the glacier flow (Figure 4A, Supplementary Figure 4). If the white surface SE of the ridge was glacier ice, then the ridge could be interpreted as some erosional bedrock feature (e.g., a volcanic dike). It could be also an ablation cone, but there are no debris bands visible on the glacier surface to support such interpretation. We are inclined to interpret the outer SE fragments of the white surface as snow patches directly adjacent to the glacier margin. Therefore, the ridge is possible a small and fragmented recessional moraine ridge. We did not show this ridge, neither possible snow patches adjacent to the glacier on the geomorphological map (Figure 3) due to uncertainties mentioned.

Glacial Processes and Landforms

The two-part structure of the Windy Glacier foreland, composed of end-moraines and a lagoon in the distal and ground



moraine, partly fluted, in the proximal part is typical of many contemporary low-relief mountain environments (Benn and Evans, 1998). The Windy Glacier foreland is somewhat similar to that of near-by Sphinx Glacier as both lack LIA terminal moraine ridges, because both terminated in the sea in the LIA maximum. The recessional moraine ridges of Windy Glacier, found beyond 1979 glacial limit, were probably formed between 1950 and 1977, because this is the time when nearby Ecology Glacier and Baranowski Glacier transgressed and formed significant push moraines (Birkenmajer, 2002; Dąbski et al., 2020).

Between 1979 and 2016 Windy Glacier front has retreated by 409 m (mean of 10 transects parallel to the glacier flow), which gives an average retreat rate of 11 m year⁻¹. This can be compared with 17 m year⁻¹ for near-by Ecology Glacier, 5–10 m year⁻¹ for Sphinx Glacier and 6.5–17 m year⁻¹ for Baranowski Glacier (Dąbski et al., 2020). The surface area loss and changes in accumulation area ratios of the glaciers is presented by Da Rosa et al. (2020). They concluded that the outlet glaciers of Warszawa Icefield slowed down their recession in the 21st century due to regional cooling, which has been shown by Oliva et al. (2016). The small fragmented ridge (partly covered with snow or ice) adjacent and parallel to the Windy Glacier margin can be interpreted as a recessional moraine ridge resulting from a still-stand, possibly linked to this cooling. Another cause of the decrease in recession rate is the transition from tidewater to land-terminating character of the glaciers snouts, which recently became a case of Windy Glacier.

Subglacially streamlined landforms mapped as small drumlins (**Figure 4A**) could be also recognized as tapering flutes after Benn and Evans (1996), because of their small length, usually less than 5 m. However, their elongation ratio is less than seven (in most cases less than four) which is typical for drumlins according to Rose (1987). Two semi-separate swarms visible on the length-to-elongation ratio diagram allowed us to draw a line boundary between the small drumlins and flutes (**Figures 4B,C**). Except for one case, all small drumlins start with a relatively large boulder. The flutings are parallel-sided with or without boulders visible on stoss sides of the flutings (**Supplementary Figure 3**). However, lack of a visible boulder can result from a till cap deposited on top of it which prevents a boulder from exposure (Benn and Evans, 1996).

The tapering shape of small drumlins together with parallel-sided character of flutes can result from differences in till rheology, where the latter forms are created in places of weaker, more dilatant deformation till (Benn and Evans, 1996). Both forms are developed side by side on the Windy Glacier ground moraine patch, therefore it can be inferred that the basal till shear strength is significantly diversified. Two eskers developed in the eastern part of the fluted moraine (**Figure 3**) can indicate that the deformation till is relatively thin and channelized conduit flow is developed at the ice-bed interface (Clark and Walder, 1994). The subglacial channels are probably R-channels (Röthlisberger, 1972) due to low ice pressure (thin glacier) and shallow bedrock. Therefore, glacially eroded bedrock fragments can undergo uneven comminution producing diversified shear strength of the basal till.

Periglacial and Paraglacial Processes and Landforms

López-Martínez et al. (2012) published an extensive spatial analysis of periglacial landforms in South Shetland Islands based on fieldwork, standard aerial photography and satellite imagery. However, they disregarded the eastern and southern margins of Warszawa Icefield on KGI (including Red Hill). López-Martínez et al. (2012) concluded that the wet periglacial environment of the archipelago allows for active freeze-thaw processes on slopes and elevated platforms, especially between 30 and 100 m a.s.l. which accords with our findings. Former studies of periglacial landforms in ASPA 128 indicated dominance of solifluction landforms, taluses and some presence of sorted patterned ground as well as frost wedges (Birkenmajer, 1980; Dutkiewicz, 1982; Kostrzewski et al., 2002; Dąbski et al., 2017). However, large-scale sorted circles are inactive or semi-active (Dutkiewicz, 1982; Dąbski et al., 2017), which testifies for the climatic amelioration since their development.

The study of Dąbski et al. (2017) performed on near-by Demay Point (**Figure 1B**) revealed sorted patterned ground already at 25.5 m GPS h., but mean elevation for this type of periglacial landforms was determined at 95.0 m GPS h. Solifluction landforms were detected on Demay Point already at 22.1 m GPS h. but mean elevation for solifluction was 85.9 m GPS h. The values of mean altitudes on the mentioned landforms are similar to those obtained in this study (95.25 m GPS h. for sorted patterned ground and 90.25 m GPS h. for solifluction landforms). The main difference between Damay Point and Red Hill is that the scarp on the latter one (**Supplementary Figure 1**) constitutes a threshold for the lowermost occurrence of the periglacial landforms, while the southern slope of Demay Point descends gently to about 20 m GPS h. allowing for significantly lower elevation of the freeze-thaw driven landforms. In both places solifluction sheets predominate among periglacial landforms (Dąbski et al., 2017). Some sorted patterned ground (e.g., large-scale sorted circles) are not developed on Red Hill at all, however, most of the sorted patterned ground looks active or semi-active as only some coarse dominants are covered by lichens or shallow tundra vegetation, while on Demay Point they look rather inactive or semi-active.

Recent liberation from glacier ice triggers quick readjustment of the landsystem to subaerial conditions which results in paraglacial processes (Ballantyne, 2002), responsible for delivery of sediments for glacial landforms to the lagoon or marine environments (Zwoliński, 2007). Da Rosa et al. (2020) emphasize the role of intense paraglacial processes acting close to the Warszawa Icefield margin. Our results fully support this finding as evidence of intense gullying and rilling (area of paraglacial erosion) is visible on 9.5 ha in the forelands of Windy Glacier – almost half of the large glacial lagoon area.

CONCLUSION

The UAV BVLOS photogrammetric survey over Windy Glacier foreland and Red Hill allowed for elaboration of a

high-resolution orthophoto and DEM on which we mapped 31 types of landforms, water bodies and other surfaces (e.g., glacier ice, snow patches, not recognized surface). The glacier margin was directly exposed to marine environment until 1979. Most area liberated from glacier ice afterward is occupied by a glacial lagoon with which the glacier lost contact and became completely land-terminated in 2006 which stopped glacial calving – the most efficient process of ablation, slowing the rate of deglaciation.

Largest terrestrial surface is occupied by fluvial (with a significant share of paraglacial rills and gullies), fluvio-glacial and littoral landforms. Between 2006 and 2016 the glacier deposited a well-developed patch of fluted moraine with small drumlins. Distinction between flutes and small drumlins is based on length-to-elongation diagram, more elongated landforms being treated as flutes.

The upper part of Red Hill, above the scarp is subject of intensive periglaciation with well-developed solifluction landforms and sorted patterned ground. The frost-sorted structures look active (due to the lack of vegetation) but there are no large-scale sorted circles as on a near-by Demay Point. Between 41 m and 47 m GPS h. we set a zone of transition between the glacial and periglacial domains.

The PW-ZOOM fixed-wing UAV BVLOS operation, followed by image processing, including the use of SfM algorithm and photointerpretation, proved to be helpful in gathering valuable geomorphological information in a location distant from the polar station where field study is difficult.

DATA AVAILABILITY STATEMENT

The original contributions presented in the study are included in the article/**Supplementary Material**, further inquiries can be directed to the corresponding author/s.

REFERENCES

- Ballantyne, C. K. (2002). Paraglacial geomorphology. *Quat. Sci. Rev.* 21, 1935–2017. doi: 10.1016/S0277-3791(02)00005-7
- Benjumea, B., Macheret, Y., Navarro, F., and Teixidó, T. (2003). Estimation of water content in a temperate glacier from radar and seismic sounding data. *Ann. Glaciol.* 37, 317–324. doi: 10.3189/172756403781815924
- Benn, D. I., and Evans, D. J. A. (1996). The interpretation and classification of subglacially-deformed materials. *Quat. Sci. Rev.* 15, 23–52. doi: 10.1016/0277-3791(95)00082-8
- Benn, D., and Evans, D. J. A. (1998). *Glaciers and Glaciations*. London: Arnold.
- Birkenmajer, K. (1980). Geology of admiralty bay, king george Island (South Shetland Islands) - an outline. *Pol. Polar Res.* 1, 29–54.
- Birkenmajer, K. (1981). Raised marine features and glacial history in the vicinity of H. Arctowski station, King George Island (South Shetland Islands, West Antarctica). *Bull. Acad. Pol. Sci. Ser. Sci. Terre* 29, 109–117.
- Birkenmajer, K. (2002). Retreat of ecology glacier, admiralty bay, king george Island (South Shetland Islands, West Antarctica), 1956–2001. *Bull. Pol. Acad. Sci. Earth Sci.* 50, 16–29.
- Chwedorzewska, K. J., and Bednarek, P. T. (2011). Genetic and epigenetic studies on populations of *Deschampsia antarctica* Desv. from contrasting

AUTHOR CONTRIBUTIONS

KK: geomorphological mapping, calculations of landforms area, and glacial recession rate, and comments to the manuscript. MD: writing of the manuscript. AZ: coordination and programming of UAV flights over Windy Glacier and preparation of source data (orthophoto) and comments to the manuscript. All authors contributed to the article and approved the submitted version.

FUNDING

Funding was provided by: (1) Project No 197810, A novel approach to monitoring the impact of climate change on Antarctic ecosystems – MONICA, funded from Norway Grants in the Polish-Norwegian Research Programme operated by the National Centre for Research and Development; (2) Project H2020-MSCA-RISE-2016: innoVation in geOspatial and 3D daTA (VOLTA), Reference GA No. 734687. H2020 VOLTA activities are supported by the Polish Ministry of Science and Higher Education in the frame of H2020 co-financed projects No. 3934/H2020/2018/2 and 379067/PnH/2017. Open-access financed by the University of Warsaw within “Excellence Initiative – Research University” Programme.

ACKNOWLEDGMENTS

The article is based on a B.Sc. diploma of KK prepared with a use of data obtained in two projects (MONICA and VOLTA) and with the support of Henryk Arctowski, Polish Antarctic Station.

SUPPLEMENTARY MATERIAL

The Supplementary Material for this article can be found online at: <https://www.frontiersin.org/articles/10.3389/feart.2021.671985/full#supplementary-material>

- environments at King George Island (Antarctic). *Pol. Polar Res.* 32, 15–26.
- Clark, P. U., and Walder, J. S. (1994). Subglacial drainage, eskers, and deforming beds beneath the Laurentide and Euroasian ice sheets. *Bull. Geol. Soc. Am.* 106, 304–314. doi: 10.1130/0016-76061994106<0304:SDEADB>2.3.CO;2
- Cook, A. J., Fox, A. J., Vaughan, D. G., and Ferrigno, J. G. (2005). Retreating glacier fronts on the Antarctic Peninsula over the past half-century. *Science* 308, 541–544. doi: 10.1126/science.1104235
- Da Rosa, K. K., Perondi, C., Veettil, B. K., Auger, J. D., and Simões, J. C. (2020). Contrasting responses of land-terminating glaciers to recent climate variations in King George Island, Antarctica. *Antarct. Sci.* 32, 398–407. doi: 10.1017/S0954102020000279
- Dąbski, M., Zmarz, A., Pabjanek, P., Korczak-Abshire, M., Karsznia, I., and Chwedorzewska, K. (2017). UAV-Based detection and spatial analyses of periglacial landforms on Demay Point (King George Island, South Shetland Islands, Antarctica). *Geomorphology* 290, 29–38. doi: 10.1016/j.geomorph.2017.03.033
- Dąbski, M., Zmarz, A., Rodzewicz, M., Korczak-Abshire, M., Karsznia, I., Lach, K. M., et al. (2020). Mapping glacier forelands based on UAV BVLOS operation in Antarctica. *Remote Sens.* 12:630. doi: 10.3390/rs12040630

- Dutkiewicz, L. (1982). Preliminary results of investigations on some periglacial phenomena on King George Island, South Shetlands. *Biul. Peryglac.* 29, 13–23.
- Fudala, K., and Bialik, R. J. (2020). Breeding colony dynamics of southern elephant seals at patelnia point, King George Island, Antarctica. *Remote Sens.* 12:2964. doi: 10.3390/rs12182964
- Goetzendorf-Grabowski, T., and Rodzewicz, M. (2017). Design of UAV for photogrammetric mission in Antarctic area. challenges in European aerospace. *Proc. Inst. Mech. Eng. G J. Aerosp. Eng.* 231, 1660–1675. doi: 10.1177/0954410016656881
- Gonera, P., and Rachlewicz, G. (1997). Snow cover at Arctowski Station, King George Island, in winter 1991. *Pol. Polar Res.* 18, 3–14.
- Kejna, M., Araźny, A., and Sobota, I. (2013). Climatic change on King George Island in the years 1948–2011. *Pol. Polar Res.* 34, 213–235.
- Kostrzewski, A., Rachlewicz, G., and Zwolinski, Z. (1998). “Geomorphological map of the western coast of Admiralty Bay, King George Island,” in *Relief, Quaternary Paleogeography and Changes of the Polar Environment*, ed. J. Repelewska-Pękalowa (Lublin: Maria Curie-Skłodowska University Press), 71–77.
- Kostrzewski, A., Rachlewicz, G., and Zwolinski, Z. (2002). The relief of the Western coast of Admiralty Bay, King George Island, South Shetlands. *Quaest. Geogr.* 22, 43–58.
- Lee, J. R., Raymond, B., Bracegirdle, T. J., Chadès, I., Fuller, R. A., Shaw, J. D., et al. (2017). Climate change drives expansion of Antarctic ice-free habitat. *Nature* 547, 49–54. doi: 10.1038/nature22996
- López-Martínez, J., Serrano, E., Schmid, T., Mink, S., and Linés, C. (2012). Periglacial processes and landforms in the South Shetland Islands (northern Antarctic Peninsula region). *Geomorphology* 15, 62–79. doi: 10.1016/j.geomorph.2011.12.018
- Marsz, A. A., and Styszyńska, A. (2000). “Główne cechy klimatu rejonu Polskiej Stacji Antarktycznej im. H. Arctowskiego (Antarktyka Zachodnia, Sztetlandy Południowe, Wyspa Króla Jerzego),” in *The main Features of the Climate in the Region of the Polish Antarctic Station H. Arctowski (West Antarctica, South Shetland Islands, King George Island) – in Polish*, eds A. A. Marsz and A. Styszyńska (Gdynia: Wyższa Szkoła Morska).
- Meredith, M. P., and King, J. C. (2005). Rapid climate change in the ocean to the west of the Antarctic Peninsula during the second half of the 20th century. *Geophys. Res. Lett.* 32:19604. doi: 10.1029/2005GL024042
- Oliva, M., Navarro, F., Hrbáček, F., Hernández, A., Nývlt, D., Pereira, P., et al. (2016). Recent regional climate cooling on the Antarctic Peninsula and associated impacts on the cryosphere. *Sci. Total. Environ.* 580, 210–223. doi: 10.1016/j.scitotenv.2016.12.030
- Osmanoğlu, B., Braun, B., Hock, R., and Navarro, F. J. (2013). Surface velocity and ice discharge of the ice cap on King George Island, Antarctica. *Ann. Glaciol.* 54, 111–119. doi: 10.3189/2013AoG63A517
- Pętliski, M., Sziło, J., MacDonell, S., Vivero, S., and Bialik, R. J. (2017). Recent deceleration of the ice elevation change of ecology Glacier (King George Island, Antarctica). *Remote Sens.* 9:520. doi: 10.3390/rs9060520
- Pudelko, R. (2003). Topographic map of the SSSI No. 8, King George Island, West Antarctica. *Pol. Polar Res.* 24, 53–60.
- Pudelko, R., Angiel, P. J., Potocki, M., Jędrejek, A. J., and Kozak, M. (2018). Fluctuation of Glacial retreat rates in the Eastern Part of Warszawa Icefield, King George Island, Antarctica, 1979–2018. *Remote Sens.* 10:892. doi: 10.3390/rs10060892
- Rachlewicz, G. (1999). Glacial relief and deposits of the western coast of Admiralty Bay, King George Island, South Shetland Islands. *Pol. Polar Res.* 20, 89–130.
- Robakiewicz, M., and Rakusa-Suszczewski, S. (1999). Application of 3D circulation model to Admiralty Bay, King George Island, Antarctica. *Pol. Polar Res.* 20, 43–58.
- Rodzewicz, M., Głowacki, D., and Hajduk, J. (2017). Some dynamic aspects of photogrammetry missions performed by “PW-ZOOM” – the UAV of Warsaw University of Technology. *Arch. Mech. Eng.* 64, 37–55. doi: 10.1515/meceng-2017-0003
- Rose, J. (1987). “Drumlins as part of a glacier bedform continuum,” in *Drumlin Symposium*, eds J. Menzies and J. Rose (Rotterdam: Balkena), 103–116.
- Röthlisberger, H. (1972). Water pressure in intra- and subglacial channels. *J. Glac.* 11, 177–203.
- Sierakowski, K., Korczak-Abshire, M., and Jadwiczak, P. (2017). Changes in bird communities of Admiralty Bay, King George Island (West Antarctica): insights from monitoring data (1977–1996). *Pol. Polar Res.* 38, 229–260. doi: 10.1515/popore-2017-0010
- Sziło, J., and Bialik, R. J. (2018). Recession and ice surface elevation changes of baranowski glacier and its impact on proglacial relief (King George Island, West Antarctica). *Geosciences* 8:355. doi: 10.3390/geosciences8100355
- Turner, J., Barrant, N. E., Bracegirdle, T. J., Convey, P., Hodgson, D. A., Jarvis, M., et al. (2014). Antarctic climate change and the environment: an update. *Polar Res.* 50, 237–259. doi: 10.1017/S0032247413000296
- Wierzbicki, G. (2009). Wiatry huraganowe w 2008 roku w Zatoce Admiralicji, Wyspa Króla Jerzego, Antarktyda Zachodnia (Storm winds in 2008 in Admiralty Bay, King George Island, West Antarctica—in Polish). *Przeg. Nauk. Inż. Kształ. Środ.* 18, 47–55.
- World Glacier Monitoring Service [WGMS] (2020). *World Glacier Monitoring Service*. Available online at: <http://wgms.ch>. (Accessed January 7, 2021).
- Young Kim, K., Lee, J., Ho Hong, M., Kuk Hong, J., Keun Jin, Y., and Shon, H. (2010). Seismic and radar investigations of Fourcade Glacier on King George Island, Antarctica. *Polar Res.* 29, 298–310. doi: 10.3402/polar.v29i3.6082
- Zmarz, A., Rodzewicz, M., Dąbski, M., Karsznia, I., Korczak-Abshire, M., and Chwedorzewska, K. J. (2018). Application of UAV BVLOS remote sensing data for multi-faceted analysis of Antarctic ecosystem. *Remote Sens. Environ.* 217, 375–388. doi: 10.1016/j.rse.2018.08.031
- Znój, A., Chwedorzewska, K. J., Androsiuk, P., Cuba-Diaz, M., Gielwanowska, I., Koc, J., et al. (2017). Rapid environmental changes in the Western Antarctic Peninsula region due to climate change and human activity. *Appl. Ecol. Environ. Res.* 15, 525–539. doi: 10.15666/aeer/1504_525539
- Zwoliński, Z. (2007). *Mobilność Materii Mineralnej na Obszarach Paraglacialnych, Wyspa Króla Jerzego, Antarktyka Zachodnia (The Mobility of Mineral Matter in Paraglacial Area, King George Island, Western Antarctica—in Polish)*. *Seria Geograficzna 74*. Poznań: Adam Mickiewicz University Press.
- Zwoliński, Z., Kejna, M., Rachlewicz, G., Sobota, I., and Szpikowski, J. (2016). “Solute and sedimentary fluxes on King George Island,” in *Source-to-Sink Fluxes in Undisturbed Cold Environments*, eds A. A. Beylich, J. C. Dixon, and Z. Zwoliński (Cambridge: Cambridge University Press), 213–237.

Conflict of Interest: The authors declare that the research was conducted in the absence of any commercial or financial relationships that could be construed as a potential conflict of interest.

Copyright © 2021 Kreczmer, Dąbski and Zmarz. This is an open-access article distributed under the terms of the Creative Commons Attribution License (CC BY). The use, distribution or reproduction in other forums is permitted, provided the original author(s) and the copyright owner(s) are credited and that the original publication in this journal is cited, in accordance with accepted academic practice. No use, distribution or reproduction is permitted which does not comply with these terms.